Nitrile Rubber – Based Nanocomposites Prepared by Melt Mixing: Effect of the Mixing Parameters on Mechanical, Dynamic-Mechanical and Creep Behavior

Bluma G. Soares, Marlucy de Oliveira, Soraia Zaioncz
Instituto de Macromolécula Professora Eloísa Mano, UFRJ

Abstract: Nanocomposites constituted by nitrile rubber matrix and Cloisite 15A (OC15A) as the organoclay were prepared by melt blending and cured with the m-phenylene-bis-maleimide (BMI)/dicumyl peroxide (DCP) system. The effect of mixing parameters on the clay dispersion was evaluated, including mixing temperature and time, and rotor speed of the internal mixer. The organoclay effectively accelerated the vulcanization reaction of NBR, which was attributed to the presence of the alkylammonium salt as the intercalant. All nanocomposites displayed improved tensile properties indicating a good reinforcing action of the clay. Also, the creep compliance was substantially reduced with the incorporation of the clay. X-ray diffraction studies showed the presence of intercalated and deintercalated clay population. The mixing parameters did not have an important effect on clay dispersion and properties of NBR-clay nanocomposites, except for the creep behavior.

Keywords: *Nitrile rubber, clay, X-ray diffraction, creep, nanocomposites, dynamic-mechanical properties, melt intercalation.*

Introduction

Polymer nanocomposites based on layered silicates have been emerged as a very promising area and have attracted great interest from academy and industry because of the improved mechanical, thermal and barrier properties that can be achieved by the addition of low amount of filler. These outstanding properties are devoted to the very high surface area, high aspect ratio and high cation exchange capacity mainly when these layered silicates belong to smectite group of clays (eg. montmorillonite, bentonite, hectorite, etc)[1]. The last characteristic is of paramount importance for the development of well dispersed polymer-clay nanocomposites since the cations naturally present in the interlayers of these silicates are easily replaced by alkylammonium cations with long aliphatic hydrocarbon chain, thus enhancing the compatibility between the organophilic clay and the polymer matrix[2].

Rubber materials are often compounded with fillers (eg. Carbon black or silica) to improve modulus, tensile strength and other important properties. The amount of these conventional fillers necessary to reach good mechanical performance is very high (between 30 to 40 phr), affecting the processability. The use of well dispersed nanoclay in rubber compounds is interesting because the desired reinforcement can be achieved without sacrifice of processing and mechanical properties[3,4]. Indeed, the presence of clay resulted in a decrease of shear viscosity in some cases[5]. In this regard, several rubber/ clay nanocomposites using for example, carboxylated nitrile-butadiene rubber[6,7], nitrile-butadiene rubber (NBR)[5,8-19], natural rubber (NR)[4,20-23], styrene-butadiene rubber (SBR)[5,19,24,25], and ethylene-propylene-diene rubber (EPDM)[26,27], among others, have been prepared via solution intercalation, melt intercalation and rubber latex compounding. Among these procedures, melt compounding is a very interesting process under the technological point of view because it does not require solvent to swell the clay, which constitutes an inherent advantage of industrial applicability and eco-friendliness. Several studies claim that highly exfoliated structures of the clay are important requirement to achieve better performance of the corresponding nanocomposites. However, fully exfoliated rubber/clay nanocomposites are very difficult to obtain, especially with the melt mixing procedure, because of the high viscosity of the rubber in the molten state[13,28]. In spite of it, several clay-based nanocomposites displayed a great improvement of mechanical performance even with non-exfoliated structures[17].

The dispersion of clay inside a rubber matrix by melt mixing depends upon several factors such as the type of intercalant[11,29], the nature of the rubber matrix[5,19,30], the compounding conditions[3] and the curing process[3,18,29,31,32]. Some researchers concluded that higher intercalated/exfoliated structures are usually achieved with more polar rubber[30]. However, Sadhu and Bhowmick have observed higher exfoliation degree with NBR containing lower amount of acrylonitrile, that is, less polar NBR[17].

The curing process has also been claimed by several authors as a very important factor governing the exfoliation/intercalation degree in rubber/clay nanocomposites. Nah et al.[9,16] observed a shift of the X-ray diffraction peak related to the basal interspacing of the organoclay towards higher 2θ values after curing the melt blended nitrile rubber-clay system. The authors have suggested that part of the intercalated component in the clay were squeezed out from the layer, giving rise to some clay aggregates. Varghese and Kocsis[4] also observed the appearance of a new diffraction peak corresponding to an interlayer distance lower than the initial organoclay basal distance after curing NR/clay system with sulfur, indicating that some clays have been confined. Zhang et al.[24] have compounded different rubbers with clay in a two roll-mill and observed that part of the clay have been intercalated by the rubber chains and another part have been re-aggregated after curing, probably because of the expulsion of some organic cations. Similar behavior has been also observed in other rubber-clay systems[19,29,33-37].

The intercalated structures of the organoclays in a rubber matrix and their spatial distribution are significantly affected by the curing parameters during the vulcanization process[31,32,36]. Several authors have investigated the effect of the different parameters involved in the vulcanization process (temperature, time and pressure) on the extent of organoclay confinement in rubber-clay nanocomposites. For example, Liang et al.[32] studied the effect of heat and pressure on intercalation structure of isobutylene-isoprene rubber/clay nanocomposites. The thermal treatment with moderate

temperature at ambient pressure (1 atm) resulted in the formation of new intercalated structures with decreased gallery height. However, increasing the temperature the exfoliated structures became dominant. The pressure also causes a decrease of the interspacing of the gallery and an increase of the coherent length of the silicate crystallites[30].

The mixing procedure affects the mechanical properties and intercalation degree of thermoplastic –based clay[1,38-41] but few papers have been devoted to this issue using rubber materials. Karger-Kocsis and Wu[3] claimed that the shear rate and mastication temperature improves the mechanical properties of the organoclay reinforced rubber. Wang et al.[42] studied the effect of some mixing parameters on the degree of exfoliation of polybutadiene-clay composite prepared by direct melt mixing of PBD, pristine clay and ammonium salt in an internal mixer. The interlayer distance slightly increased with increasing of mixing temperature, but too high temperature (110 °C) resulted in a decrease of the gallery interspacing.

The present work aims to investigate the effect of some mixing parameters on the mechanical, and dynamic- mechanical properties of NBR-organoclay nano-composites prepared by melt blending and try to establish a relationship between these results and the intercalation degree of clay in these composites by using X-ray diffraction technique. All samples have been submitted to the same curing treatment using peroxide-based system, so that the differences found in the samples were mainly related to the mixing conditions.

Experimental

Materials

Nitrile rubber (NBR) [acrylonitrile (ACN) content = 45 % and Mooney viscosity (ML (1+4) at 100 °C) = 60] was kindly supplied by Petroflex Ind. Com. S.A. Brazil. The organoclay used in this study was Cloisite ® 15A (OC15A) (a natural montmorillonite modified with dimethyl-ditallow quaternary ammonium salt with a CEC of 125 mequiv/100g,) supplied by Southern Clay Products, USA. N,N'-m-phenylene-bis-maleimide (BMI) was purchased by Dupont Dow Elastomers with the trade code HVA-2. Dicumyl peroxide (DCP) was supplied by Retilox Química Especial Ltda, Brazil.

Preparation of nanocomposites

NBR/organoclay nanocomposites were prepared in a Brabender Plastograph equipped with a W50 EHT internal mixer using banbury blades, operating at different rotor speed and a fill factor of 0.85. The NBR was first masticated at different temperatures for 2 minutes, and then mixed with 2.5 phr of (OC15A) for different times. The compounded rubber was then transferred to an open two roll mill and the curatives (DCP and BMI in a proportion of 1.0 to 1.0 phr), were added.

The samples were compression molded in a hydraulic press at 170 °C at a pressure of 5 MPa. The molding time was adjusted according to the optimum cure time (ASTM D 2084-81 method), as determined from an oscillating disk rheometer (ODR; Tecnologia Industrial – model T100; Argentina) with an oscillating angle of 1°. The optimum cure time was established as the time to reach 90% of the maximum torque. The test specimens (2.0 mm thick) for stress-strain analysis were cut from the molded slabs. The test specimens for XRD measurements were prepared from molded slabs of approximately 0.5 mm.

Characterization and testing

X-ray diffraction (XRD) studies were performed on a Rigaku Ultima IV X-ray diffractometer (40 kV, 20 mA) in the range of 2θ = 0.5-10 degree. The d-spacing of the clay particles was calculated with the Bragg's equation:

$$n\lambda = 2d.\sin\theta \tag{1}$$

where λ is the wavelength of the X-ray (for the Cu target used here, the λ value is 1.5418 Å), d is the interplanar distance and θ is the angle of incident radiation.

Tensile testing of the samples has used dumb bell-shaped test specimens according to DIN 53504 – type S2 method. The measurements were performed in a Universal testing machine, Instron model 5569, at a crosshead speed of 200 mm/min, and 25 °C.

For oil uptake measurements, the test specimens were immersed in a mineral oil at 100 °C for 22 hours. The test specimens were then removed from the oil, wiped with tissue paper to remove the excess oil from the surface and weighted. Percentage mass swell was then calculated as follow:

$$Change\ in\ mass = \frac{W_2 - W_1}{W_1} x100 \tag{2}$$

where W_1 and W_2 are the weight of the samples before and after immersion, respectively.

Short-time creep tests were carried out using the methodology described by Siengchin and Karger-Kocsis[43,44], in a DMA Q800 apparatus (TA Instruments), using the tensile mode at 25 °C. The creep and recoverable compliance were determined as a function of time (t_{creep} = 10 minutes and $t_{recovery}$ = 30 minutes) It was applied a tensile stress of 0.1 MPa. For these experiments, the specimen dimensions were $3 \times 1 \times 0.5$ mm³ (width × length × thickness).

Results and Discussion

XRD studies

The effect of mixing parameters on the organoclay dispersion inside the NBR matrix was evaluated by X-ray diffractometry, taken at 2θ range from 0.6 to 10°, whose main profiles are illustrated in Figure 1. The XRD analysis of pure organoclay OC15A was also included for comparison. Pure OC15A displayed two main diffraction peaks at 2θ = 2.7° and 4.0°, corresponding to interlayer spacings of 33 Å and 22 Å, respectively. The presence of two non resolvable peaks can be attributed to the different size of the alkyl chain in the alkylammonium salt as the intercalant and also the different amount of intercalant in the clay platelets. In addition, it is possible to observe another small peak at 2θ = 6.8° which is typical of the pristine MMT Na⁺. This diffraction peak profile shows that the commercial organoclay does not present a well-defined order of the silicate layers and is characterized by the presence of galleries containing different size of carbon chain and different amount of intercalant. These features and the large average interlayer spacing contribute for a good intercalation of the polymer chain inside its galleries.

The NBR-clay nanocomposites displayed several diffraction peaks, indicating that the clay platelets are not completely exfoliated. In addition, it is possible to observe different clay populations: some of them appeared at 2θ lower than the original clay showing interlayer spacings larger than that observed for the OC15A organoclay, indicating an intercalated / exfoliated dispersion state. Other organoclay populations inside the nanocomposites exhibited
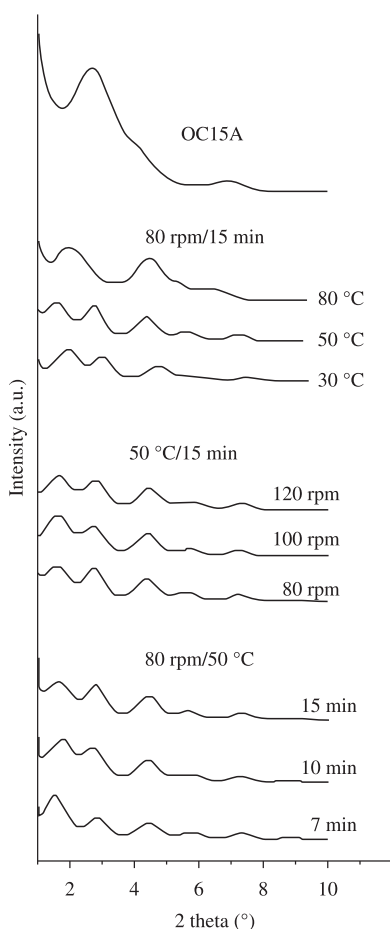
Figure 1. XRD patterns of the melt blended NBR/clay nanocomposites as function of the mixing parameters.

Table 1. X-ray diffraction data of NBR-clay nanocomposites as a function of the mixing parameters.

Mixing temperature (°C)	Rotor speed (rpm)	Mixing time (minutes)	Interlayer distance (Å)	Amount of clay population (%)
			33	67
	Cloisite 15A		22	21
			13	12
30	80	15	49	33
			30	27
50	80	15	55	24
			32	28
80	80	15	41	48
			20	37
50	80	15	55	24
			32	28
50	100	15	55	37
			33	29
50	120	15	55	30
			32	31
50	80	7	59	41
			31	20
50	80	10	52	29
			33	28
50	80	15	55	24
			31	28

interlayer spacings smaller than that of the original organoclay used in these composites, suggesting that some amount of the original intercalant were removed out from the clay galleries, resulting in a collapse of the intercalated structure, as was also observed by other authors[4,24,31,32,36]. This claim is based on the fact that the values found for the basal reflections do not fit to the corresponding (002) or (003) harmonic reflections either in respect to their positions or relative intensities. Table 1 summarizes the amount of the intercalated clay (with d-spacing larger than 22 Å) as a function of the mixing parameters. The proportion of different populations of the intercalated clay was estimated from the deconvolution of the peaks, using free peak fitting software, called fityk[1], by relating the area of each diffraction peak with the total area of the peaks[45]. Almost all samples presented proportions of intercalated clay species (interlayer spacing larger than 22 Å) higher than 50%. However, the nanocomposite performed at 80 °C presented higher proportion of deintercalated clay (confined clay) than the other nanocomposites probably because of the possible decomposition of the intercalant (quaternary ammonium salt), through the reaction known as Hofmann elimination, as pointed out by other authors[46]. By using the mixing temperature corresponding to 50 °C, it was

---

[1] fityk is a program for nonlinear fitting of analytical functions (especially peak-shaped) to data (usually experimental data) and it was friendly downloaded at http://www.unipress.waw.pl/fityk/.

observed a clay population with the highest interlayer distance (55 Å). At this temperature, the rotor speed and mixing time did not present any significant influence on the XRD profile and the percentage of intercalated clay.

Curing parameters and physico-mechanical properties

The effect of mixing parameters on the curing characteristics and mechanical properties is summarized in Table 2. The presence of 2.5 phr of oganoclay resulted in a decrease of the optimum curing time whereas the scorch time did not change the values. These results suggest an increase of the curing rate promoted by the quaternary alkylammonium salt present as the intercalant for the organoclay. Similar results have been observed by other authors[9,28]. The maximum torque also increased with the presence of clay.

The physical properties of NBR composites are also summarized in Table 2, as a function of the mixing parameters. The presence of low amount of clay, as 2.5 phr, resulted in a significant improvement of tensile strength and elongation at break, indicating an important reinforcing effect of the clay. Similar behavior has been observed by other authors who have attributed to a synergistic action of platelet orientation and chain slippage[24,29]. As far as the mixing parameters are concerned, there is no significant change in the mechanical properties of the nanocomposites prepared at different ways. The only composite that presented a decrease of the ultimate tensile

strength when compared to the other nanocomposites was that processed at 80 °C. This sample also presented the lowest amount of intercalated clay, confirming that good mechanical properties are usually related to a good clay dispersion inside the rubber matrix.

The nanocomposites presented higher percentage of oil uptake, indicating lower oil resistance, when compared to the gum sample, which may be attributed to the presence of the long aliphatic hydrocarbon chain in the organoclay, providing a good affinity towards mineral oil.

Creep behavior

The creep behavior is very sensitive to the presence of nanofiller[47]. This technique has been also employed in our studies to evaluate the influence of mixing parameters during the melt blending the NBR-clay nanocomposites. Figure 2 displays the creep compliance behavior and strain recovery (in terms of strain percentage) of the vulcanized NBR and their filled nanocomposites as a function of the mixing parameters. All composites present significant lower creep compliance values compared to the pure NBR gum. Also the strain recovery of all nanocomposites was very good and comparable to the pure NBR.

The compliance values were not significantly affected by the mixing temperature (Figure 2a). However, the sample prepared at 80 °C (curve c), which displayed the lowest amount of intercalated clay, also presented the worst strain recovery, probably because of some intercalant decomposition at higher temperature.

The rotor speed exerted a significant influence on creep compliance. The lowest variation was observed on sample prepared at 100 rpm. This sample also presented the highest strain recovery, that is, the best elastic recovery. The amount of intercalated clay in this sample is also higher. The mixing time also exerted some influence on the creep behavior: shorter processing time (7 minutes) decreased the creep compliance and displayed the best creep recovery It is important to point out that some nanocomposites, processed at different conditions, presented a creep recovery more rapidly than the pure NBR gum. These results indicate that the presence of well dispersed clay in nanosize dimensions is very important to achieve good mechanical properties and good resistance to creep, as well as good recovery. This behavior is attributed to the large superficial area of the nanofillers which contributes for an increase of the interaction filler-matrix.

Table 2. Curing characteristics and mechanical properties of vulcanized NBR and their composites with 2.5phr of organoclay prepared with different mixing parameters.

Material	Mixing parameters			MH (lb.in)	t_{s1} (minutes)	t_{90} (minutes)	σ_B (MPa)	ε_B (%)	Modulus at 100% (MPa)	Oil uptake (%)
	Rotor speed (rpm)	Mixing temperature (°C)	Mixing time (minutes)							
NBR	80	80	15	23	1.1	10.5	2.5 ± 0.1	450 ± 32	0.64 ± 0.02	0.50
	Variation of mixing temperature									
	80	30	15	25	1.2	8.1	5.1 ± 0.7	650 ± 93	0.90 ± 0.07	2.08
NBR/clay	80	50	15	28	1.2	8.1	6.1 ± 0.8	710 ± 87	0.90 ± 0.05	1.85
	80	80	15	27	1.2	7.6	4.1 ± 0.5	730 ± 70	0.68 ± 0.01	1.34
	Variation of rotor speed									
	80	50	15	28	1.2	8.1	6.1 ± 0.8	710 ± 87	0.90 ± 0.05	1.85
NBR/clay	100	50	15	27	1.1	8.0	5.7 ± 0.3	720 ± 20	0.83 ± 0.01	1.92
	120	50	15	26	1.1	7.2	7.2 ± 1.0	740 ± 90	0.97 ± 0.02	1.78
	Variation of mixing time									
	80	50	7	27	1.1	7.3	5.8 ± 1.5	640 ± 20	0.98 ± 0.1	2.05
NBR/clay	80	50	10	27	1.1	7.3	6.1 ± 0.6	740 ± 55	0.84 ± 0.04	2.01
	80	50	15	28	1.2	8.1	6.1 ± 0.8	710 ± 87	0.90 ± 0.05	1.85

M_H = maximum torque; t_{s1} = sorch time; t_{90} = optimum curing time; σ_B = ultimate tensile strength; ε_B = elongation at break.
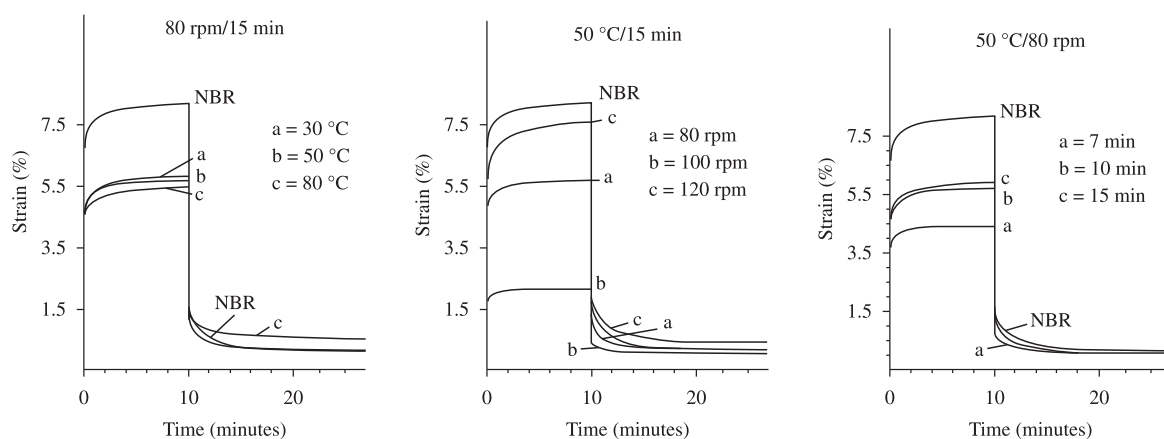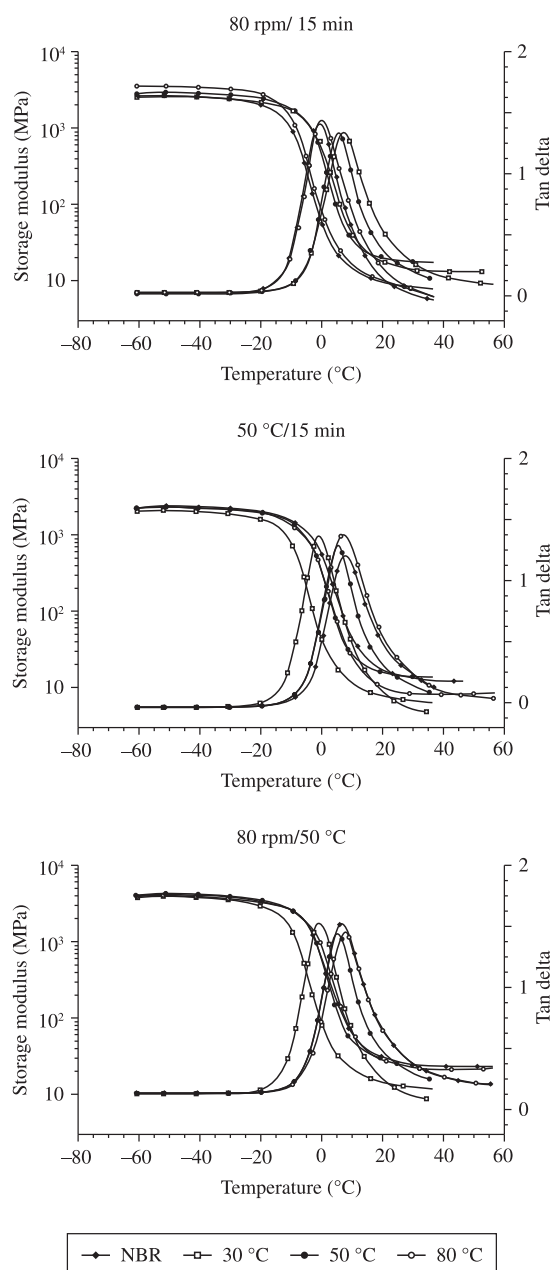

Figure 2. Creep compliance behavior and strain recovery of vulcanized NBR and the OC15A/NBR nanocomposites prepared by melt intercalation process at different mixing parameters.

Dynamic-mechanical analysis

The effect of the mixing processing on the dynamic-mechanical properties was also evaluated, in terms of storage modulus and tan delta versus temperature. All NBR-based nanocomposites displayed higher storage modulus below glass transition temperature and higher glass temperature than those found for pure vulcanized NBR sample, indicating reinforcing action of the clay. This effect is illustrated in Figure 3. Among the nanocomposites, the mixing parameter did not influence these properties.

Figure 3. Dynamic mechanical analysis of vulcanized NBR and the OC15A/NBR nanocomposites prepared by melt intercalation process at different mixing parameters.

Conclusion

Based on the results obtained in this report, one can conclude that the presence of low amount of clay, as 2.5 phr, in NBR vulcanizates prepared by melt mixing, resulted in a significant improvement of tensile properties mainly the ultimate tensile strength and elongation at break, indicating a good reinforcing action of the clay. Also the creep compliance was substantially reduced with the incorporation of the clay. In some cases, the strain recovery of nanocomposites was more rapidly than the pure NBR gum. All nanocomposites are transparent, indicating that the aggregation of the clay in large particles was not important. The XRD patterns of the vulcanized nanocomposites presented similar profiles, with different clay populations in the intercalated and deintercalated forms. In addition, the diffraction peaks are somewhat broad indicating a decrease of the degree of coherent silicate order. The mixing parameters did not exert any significant influence on the intercalation degree of organoclay in NBR-clay nanocomposites, except when higher mixing temperature was employed. In this case, higher temperature resulted in a deintercalation process of the organoclay in higher extent.

Regarding the dynamic mechanical parameters, the presence of clay also increases the storage modulus and glass transition temperature confirming the nanoreinforcing action of the clay.

Acknowledgements

References

1. Goettler, L. A.; Lee, K. Y. & Thakkar, H. - Polym. Rev., **47**, p.291 (2007).

2. Pavlidou, S. & Papaspyrides, C. D. - Prog. Polym. Sci., **33**, p.1119 (2008).

3. Karger-Kocsis, J. & Wu, C. M. - Polym. Eng. Sci., **44**, p.1083 (2004).

4. Varghese, S. S. & Karger-Kocsis J. - J. Appl. Polym. Sci., **91**, p.813 (2004).

5. Sadhu, S. & Bhowmick, A. K. - J. Polym. Sci. Phys., **43**, p.1854 (2005).

6. Fritzsche, J.; Das, A.; Jurk, R.; Stockelhuber, K. W.; Heinrich, G. & Kluppel, M. - Express Polym. Lett., **2**, p.373 (2008).

7. Das, A.; Stockelhuber, K. W. & Heinrich, G. - Macromol. Chem. Phys., **210**, p.189 (2009).

8. Wu, Y-P.; Jia, Q-X.; Yu, D-S. & Zhang, L-Q.- J. Appl. Polym. Sci., **89**, p.3855 (2003).

9. Choi, D.; Kader, M. A.; Cho, B-H.; Huh, Y-I. & Nah, C. - J. Appl. Polym. Sci., **98**, p.1688 (2005).

10. Nah, C.; Ryu, H. J.; Kim, W. D. & Choi, S-S. - Polym. Adv. Technol., **13**, p.649 (2002).

11. Kim J. T.; Oh, T. S. & Lee, D. H. - Polym. Int., **52**, p.1058 (2003).

12. Kim, J. T.; Oh, T-S. & Lee, D-H. - Polym. Int., **53**, p.406 (2004).

13. Nah, C.; Ryu, H. J.; Han, S. H.; Rhee, J. M. & Lee, M-H. - Polym. Int., **50**, p.1265 (2001).

14. Kim, J-T.; Lee, D-Y.; Oh, T-S. & Lee, D-H. - J. Appl. Polym. Sci., **89**, p.2633 (2003).

15. Liu, L.; Jia, D.; Luo, Y. & Guo, B. - J. Appl. Polym. Sci., **100**, p.1905 (2006).

16. Nah, C.; Ryu, H. J.; Kim, W. D. & Chang, Y-W. - Polym. Int., **52**, p.1359 (2003).

17. Sadhu, S. & Bhowmick, A.K. - J. Polym. Sci. Phys., **42**, p.1573 (2004).

18. Das, A.; Jurk, R.; Stockelhuber, K. W. & Heinrich, G. - Macromol. Mater. Eng., **293**, p.479 (2008).

19. Ma, Y.; Wu, Y-P.; Zhang, L-Q. & Li, Q-F. - J. Appl. Polym. Sci., **109**, p.1925 (2008).

20. Sun, Y.; Luo, Y. & Jia, D. - J. Appl. Polym. Sci., **107**, p.2786 (2008).

21. Madhusoodanan, K. N. & Varghese, S. - J. Appl. Polym. Sci., **102**, p.2537 (2006).

22. Jurkowska, B.; Jurkowski, B.; Oczkowski, M.; Pesetskii, S. S.; Koval, V. & Olkhov, Y. A. - J. Appl. Polym. Sci., **106**, p.360 (2007).

23. Li, P.; Wang, L.; Song, G.; Yin, L.; Qi, F. & Sun, L. - J. Appl. Polym. Sci., **109**, p.3831 (2008).

24. Wu, Y-P.; Ma, Y.; Wang, Y-Q. & Zhang, L-Q. - Macromol. Mater. Eng., **289**, p.890 (2004).

25. Liao, M.; Zhu, J.; Xu, H.; Li, Y. & Shan, W. - J. Appl. Polym. Sci., **92**, p.3430 (2004).

26. Chang, Y-W.; Yang, Y.; Ryu, S. & Nah, C. - Polym. Int., **51**, p.319 (2002).

27. Tan, H. & Isayev, A. I. - J. Appl. Polym. Sci., **109**, p.767 (2008).

28. Mousa, A. & Karger-Kocsis, J. - Macromol. Mater. Eng. **286**, p.260 (2001).

29. Gatos, S.; Sawanis, N. S.; Apostolov, A. A.; Thomann, R. & Karger-Kocsis, J. - Macromol. Mater. Eng., **289**, p.1079 (2004).

30. Liang, Y-R.; Cao, W-L.; Zhang, X-B.; Tan, Y-J.; He, S-J. & Zhang, L-Q. - J. Appl. Polym. Sci., **112**, p.3087 (2009).

31. Lu, Y-L.; Liang, Y-R.; Wu, Y-P. & Zhang, L-Q. - Macromol. Mater. Eng., **291**, p.27 (2006).

32. Liang, Y-R.; Ma, J.; Lu, Y-L.; Wu, Y-P.; Zhang, L-Q. & Mai, Y-W. - J. Polym. Sci. Polym. Phys., **43**, p.2653 (2005).

33. Wan, C.; Dong, W.; Zhang, Y. & Zhang, Y. - J. Appl. Polym. Sci., **107**, p.650 (2008).

34. Gatos, K. G.; Thomann, R. & Karger-Kocsis, J. - Polym. Int., **53**, p.1191 (2004).

35. Gatos, K. G. & Karger-Kocsis, J. – Polymer, **46**, p.3069 (2005).

36. Gatos, K. G.; Szazdi, L.; Pukanszky, B. & Karger-Kocsis, J. - Macromol. Rapid. Comun., **26**, p.915 (2005).

37. Kashani, M. R.; Hasankhani, H. & Kokabi, M. - Iranian Polym. J., **16**, p.671 (2007).

38. Rodolfo Jr, A. & Mei, L. H. - Polímeros, **19**, p.1 (2009).

39. Dasari, A.; Yu, Z-Z. & Mai, Y-W. – Polymer, **46**, p.5986 (2005).

40. Dennis, H. R.; Hunter, D. L.; Chang, D.; Kim, S.; White, J. L. & Cho, J. W. – Polymer, **42**, p.9513 (2001).

41. Davis, C. H.; Mathias, L. J.; Gilman, J. W.; Schiraldi, D. A. & Trulove, P. - J. Polym. Sci. Phys., **40**, p.2661 (2002).

42. Wang, S.; Zhang, Y.; Peng, Z. & Zhang, Y. - J. Appl. Polym. Sci., **98**, p.227 (2005).

43. Siengchin, S. & Karger-Kocsis, J. - Macromol. Rapid. Commun. **27**, p.2090 (2006).

44. Siengchin, S., Karger-Kocsis, J. & Thomann, R. - Express Polym. Lett., **2**, p.746 (2008).

45. Soares, B. G.; Oliveira, M.; Zaioncz, S.; Gomes, A. C. O.; Silva, A. A.; Santos, K. S.; Mauler, R. S. – J. Appl. Polym. Sci. in press.

46. Gilman, J. W. – Appl. Clay. Sci., **15**, p.31 (1999).

47. Karger-Kocsis, J. & Zhang, Z. - "Mechanical Properties of Polymers Based on Nanostructure and Morphology", CRC Press, Boca Raton, (2005).